Preparation and Properties of a Poly(2-cyano-1,4-phenylene terephthalamide)/Layered Silicate Nanocomposite

Soo-Young Park,[1] Seung-Woo Lee,[1] Tae-Jin Oh[2]

[1]*Department of Polymer Science, Kyungpook National University, Buk-gu, Daegu 702–701, Korea*
[2]*Department of Textile System Engineering, Kyungpook National University, Buk-gu, Daegu 702–701, Korea*

Received 25 October 2005; accepted 21 February 2006
DOI 10.1002/app.24411
Published online in Wiley InterScience (www.interscience.wiley.com).

ABSTRACT: The *in situ* polymerization method was used to prepare a poly(2-cyano-1,4-phenylene terephthalamide)/layered silicate nanocomposite with organically-modified clay (Cloisite® 30B, southern clay), which was spun into well-oriented fibers and cast into film in the lyotropic and isotropic state, respectively. The degradation temperature of the nanocomposite (~550°C) was similar to that of poly (2-cyano-1,4-phenylene terephthalamide) and its strength (and modulus) linearly increased with the amount of the layered silicate in the nanocomposite. The intercalated structure was observed using transmission electron microscopy and X-ray diffraction with an increase in *d*-spacing of the layered silicate from 18.7 Å (the organically modified layered silicate; cliosite 30B) to 21.1 Å (nanocomposite). The layered silicate in the nanocomposite was well oriented during fiber spinning and film casting. The normal of the surface of the layered silicate was perpendicular to the fiber axis and the surface of the cast film. © 2006 Wiley Periodicals, Inc. J Appl Polym Sci 102: 640–645, 2006

Key words: poly(2-cyano-1,4-phenylene terephthalamide); kevlar; layered silicate; clay; nanocomposite

INTRODUCTION

Polymer/layered silicate nanocomposite (PLSN) has gained a great deal of attention since Toyota researchers first demonstrated a stunning improvement of its mechanical properties, when compared with pristine nylon 6. Most notable is the unexpected suite of property enhancements obtained from the addition of a few weight percentage of layered silicate, such as the retention of impact strength, increased atomic oxygen resistance, and an improved ablative performance.[1–8] The PLSN systems, however, have not been applied to high-performance polymers such as poly(*p*-phenylenebenzobisthiazole), poly(*p*-phenylenebenzobisoxazole) (PBO), and poly(*p*-phenyleneterephthalamide) (PPTA; DuPont Kevlar®). Such polymers are usually soluble only in strong acids such as polyphosphoric acid and/or sulfuric acid, which destroy the organically modified layered silicates. PPTA has excellent thermal and thermoxidative stability, as well as exceptional tensile strength and tensile modulus when it is spun into fiber. These properties are attributable to chain stiffness and a high degree of molecular orientation and crystallinity, which are achieved by dry-jet-wet-spinning from a liquid crystalline solution of PPTA in hot 100% sulfuric acid.[9–12] The use of sulfuric acid as the solvent, however, results in some molecular weight degradation, which leads to less than optimum physical properties. Also, it leads to difficulties in environmental and process control. Chemical modification of PPTA, to improve solubility, has been attempted by adding halogens or other chemical substituents on the phenylene rings.[13] Poly(2-cyano-1,4-phenylene terephthalamide) (CN-PPTA), in which a cyano group is substituted at the *p*-phenylene diamine segment, was used in the current study. This polymer is soluble in polar organic solvents that contain small amounts of inorganic salts, for example, dimethylacetamide, which contains 2% LiCl.[14,15] The tensile strength and modulus of the CN-PPTA fibers that are spun in the lyotropic state are comparable to those of Kevlar even though bulky cyano groups have been substituted.[14,15] Thus, CN-PPTA has the potential to be used in high-performance nanocomposite system, because when soluble, CN-PPTA can be used as a matrix material for the PLSN system.

The current study developed the *in situ* synthesis of a CN-PPTA/layered silicate nanocomposite in an organically modified layered silicate solution. Herein, we report on the properties and structures of the CN-PPTA/layered silicate nanocomposite. To our knowledge, this is the first report regarding PLSN systems using Kevlar and its derivatives.

Correspondence to: S.-Y. Park (psy@knu.ac.kr).
Contract grant sponsor: Basic Research Program of the Korea Science and Engineering Foundation; contract grant number: R08–2003-000–10338–0 (2003).

EXPERIMENTAL

The *in situ* polymerization of a CN-PPTA/layered silicate nanocomposite

Poly(2-cyano-1,4-phenylene terephthalamide) CN-PPTA was synthesized as described in the US patent.[16] A CN-PPTA/layered silicate nanocomposite, with different clay ratios on the weight of polymer, was prepared by the *in situ* polymerization of CN-PPTA with terephthaloylchloride (TPC) in a sonicated, well-dispersed, organoclay cloisite® 30B (southern clay©) solution of *N*-methylpyrrolidone (NMP). The composite was prepared as follows: 100 mL of NMP and 1.202 g of cloisite 30B (7.5% on the weight of CN-PPTA) were added to a four-necked, round-bottom flask equipped with a mechanical stirrer, and a nitrogen inlet and outlet and sonicated for 1 h in an ultrasound bath (40 kHz). Cyano PPD (*p*-phenylenediamine) (8.104 g) was added to the sonicated cloisite 30B solution and stirred at room temperature until complete dissolution. The solution was cooled to 5°C in an ice bath. TPC (6.177 g) was added to this solution with rapid stirring for 10 min, giving rise to an increase in the temperature of up to 30°C. The solution was cooled to 5°C, and then, TPC (6.177 g) was added with vigorous stirring. This leads to a rapid increase in the viscosity and finally solidification of the reaction product in a few minutes. An equimolar amount of Li_2CO_3 (0.4497 g) was added to the solidified reaction product to neutralize HCl that was generated during the reaction. After constant stirring for several hours, a liquid crystalline polymer solution of low viscosity was formed. The evidence for the presence of nematic phase was obtained by observing an optical birefringence of a dope sample examined under a crossed-polarizing optical microscope.

Air gap spinning and film formation

LiCl (1.755 g) was added to the lyotropic liquid crystalline polymer solution, to increase its viscosity for air-gap spinning. The anisotropic CN-PPTA/organoclay dope, which contained 13 wt % of the polymer and 5.5 wt % of LiCl, was deareated at 60°C and filtered through a 400-mesh stainless-steel screen. It was spun at room temperature with a draw ratio of 8 through a 10-mm air gap into a distilled water bath at temperatures below 10°C. Subsequently, the fiber was soaked in a large amount of distilled water for several days to remove any residual solvents. The fiber was dried under tension at 135°C for 1 h. Also, the isotropic solution was cast into film on the glass substrate by rolling the glass rod taped with the same amount of aluminum film at both ends of the rod on to the glass substrate. This was done to maintain the constant thickness of the film. The film was soaked and dried by using the same method of the fiber.

General characterizations

Optical microscopy on the polymer dope was performed using a Leitz polarizing microscope. Thermogravimetric analyses (TGA) of the bulk polymer samples were performed in nitrogen using TG/DTA 320 (Seiko Instruments, Japan) at a heating rate of 10°C/min. For tensile testing, the CN-PPTA fiber was dried under tension at a temperature of 135°C for 1 h. The tensile modulus and the strength were determined using a vibrascopic single-fiber tensile testing machine using Vibrojet 2000 (Lenzing Instruments).

Transmission electron microscopy

Transmission electron microscopy (TEM) images were obtained using a Hitachi H-7600 microscope with an accelerating voltage of 100 kV. Ultrathin sections (~70 nm) were prepared orthogonal to the film surface using an American Optical Ultracut microtome.

X-ray characterization

Film specimens for the three-dimensional X-ray analysis were prepared by stacking the ~1.5-mm wide films, such that the X-ray specimen was ~1 mm thick. Wide-angle X-ray diffraction patterns were recorded on a phosphor image plate (Molecular Dynamics©) in a Statton camera with the beam aligned normal (the ND pattern) and parallel (the TD pattern), to the film surface. A Rigaku rotating anode X-ray generator, operated at 40 kV and 240 mA, produced Cu Kα radiation, which was monochromated with a flat monochromator (Huber © Model 151). The sample-to-film distance was calibrated by SiO_2 powders. The one-dimensional small angle X-ray data were recorded by using SAXSess (Anton Parr©).

RESULTS AND DISCUSSION

CN-PPTA/layered silicate nanocomposite

Figure 1 shows the picture of a fiber of CN-PPTA/3 wt % layered silicate observed through the polarized optical microscope under a cross-polarizing filter. The birefringence in Fig. 1 indicates that they were well oriented because of spinning from the nanocomposite dope in a lyotropic state.

Figure 2 shows the TGA thermograms of the CN-PPTA/layered silicate nanocomposites, with different amounts of layered silicate. The degradation temperatures were around 550°C and did not change with the addition of layered silicate. A slight increase in the degradation temperature of the CN-PPTA/layered silicate nanocomposite, compared with that of the pure CN-PPTA, may have been due to the already high degradation temperature of CN-PPTA. It has been reported that the thermal stability of the PBO/clay

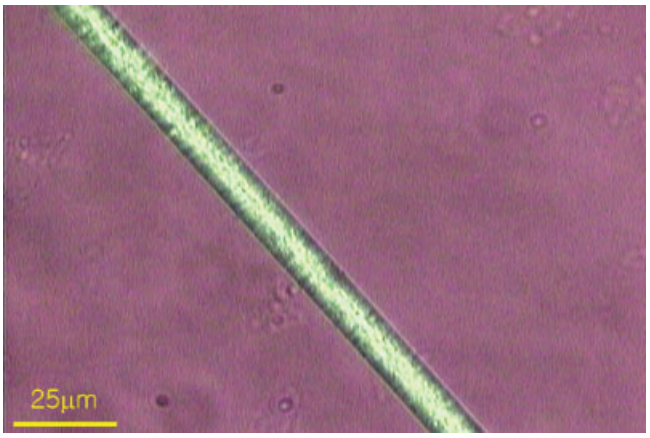

Figure 1 Picture of a fiber of CN-PPTA/3 wt % clay layered silicate observed through the polarized optical microscope under a cross polarizing filter. [Color figure can be viewed in the online issue, which is available at www.interscience.wiley.com.]

nanocomposites increased slightly with the addition of organoclay.[17] This temperature indicates that this PLSN can be used for high-temperature applications.

Table I shows a summary of the mechanical properties of the spun fibers. The elongations are nearly constant, while the strengths almost linearly increase with the amount of the layered silicate. These values are for the samples made by the laboratory spinning machine, so the values would increase from the process optimization. From the linear least-square fit of the graph of the strength versus the amount of the layered silicate, the slope was 1.31 g/day (per 1 wt % layered silicate) and the intercept was the 3.44 g/day (which would be the strength of CN-PPTA with a similar molecular weight). The value of 3.44 g/day for CN-PPTA seems to be low, which indicates that the molecular weight of CN-PPTA in the nanocomposite is low compared with that of the conventional CN-PPTA synthesized in the same conditions. The molecular weights of the CN-PPTA/layered silicate nanocomposites could not be measured because of the layered silicate component in the polymer. The strength of the CN-PPTA/7.5 wt % layered silicate nanocomposite is nearly twice that of the CN-PPTA/2.5 wt % layered silicate nanocomposite. This result strongly suggests that a small amount of layered silicate has a significant effect on the strength of the nanocomposite.

TABLE I
Summary of the Mechanical Properties of the Spun Fibers with Different Amounts of Layered Silicate

Layered silicate (wt %)	Elongation (%)	Strength (g/d)
2.5	3.2	6.87
5	3.7	9.72
7.5	3.7	13.44

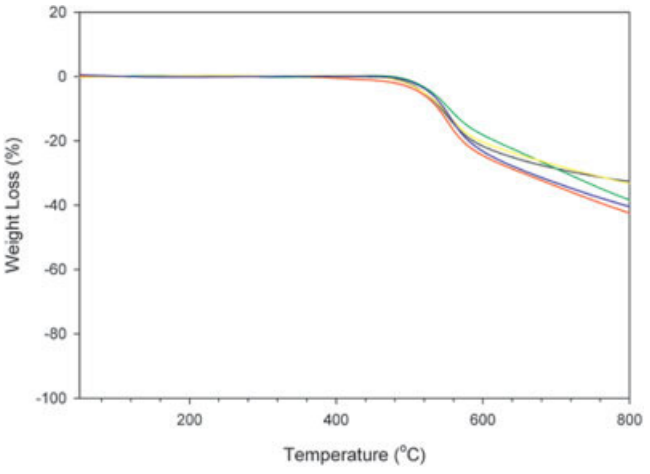

Figure 2 TGA thermograms of the CN-PPTA/layered silicate nanocomposites with different amounts of layered silicate. Blue, CN-PPTA/0 wt % layered silicate; yellow, CN-PPTA/2.5 wt % layered silicate; green, CN-PPTA/5 wt % layered silicate; red, CN-PPTA/7.5 wt % layered silicate; black, CN-PPTA/10 wt % layered silicate. [Color figure can be viewed in the online issue, which is available at www.interscience.wiley.com.]

Dynamic mechanical analysis

Figure 3 shows a DMA theromogram of a single fiber of the CN-PPTA/5 wt % layered silicate nanocomposite. The storage and loss moduli changed little until 400°C, indicating that the mechanical properties were maintained at a high temperature. The nanocomposite, with other amounts of layered silicates, showed

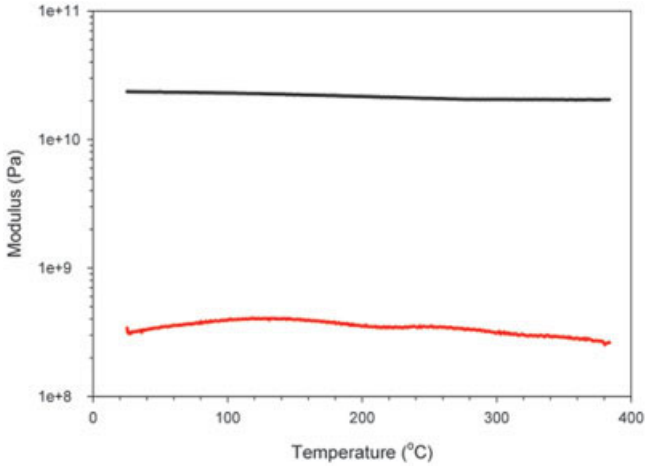

Figure 3 DMA theromogram of a single fiber of the CN-PPTA/5 wt % layered silicate nanocomposite. Black, storage modulus; red, loss modulus. [Color figure can be viewed in the online issue, which is available at www.interscience.wiley.com.]

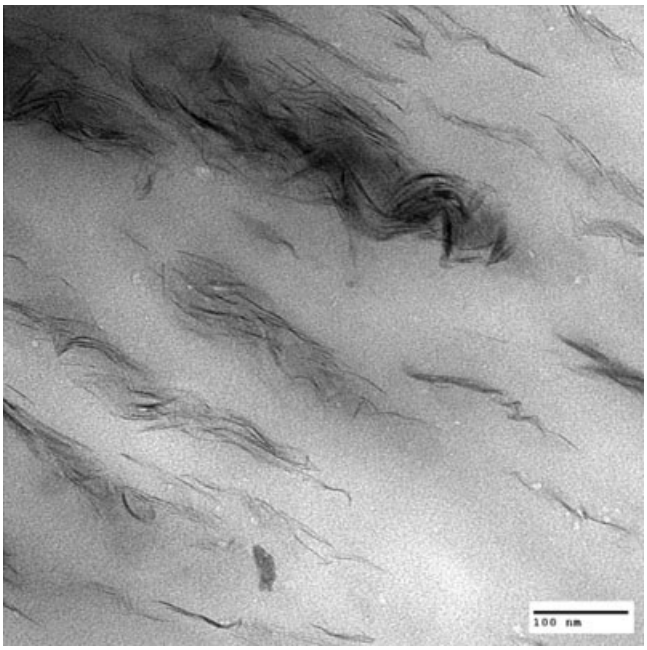

Figure 4 The transmission electron micrographs of the pressed film of the CN-PPTA/5 wt % layered silicate nanocomposite, sectioned along the thickness direction with ×30,000 magnification.

similar behavior. The tan δ value is low and is at a constant of ~0.014 from room temperature to 380°C. This indicates that high elastic properties were maintained even at ~400°C. The measured temperature range was from room temperature to 389°C, and the stability of the mechanical properties extended above 400°C, when the measured temperature increased.

Structure of the CN-PPTA/layered silicate nanocomposite

Figure 4 shows the transmission electron micrographs of the cast film of the CN-PPTA/5 wt % layered silicate nanocomposite, which is sectioned along the thickness direction. The surface of the layered silicates is oriented along one direction, which is parallel to the film surface. The layered silicates are well dispersed throughout the film and the galleries of the layered silicates are slightly open, especially, at the edge of the layered silicate. This result indicates that the structure of the layered silicate in the nanocomposite is intercalated although the galleries have some distributions in the gap. The layered silicates are not straight but wavy, especially at the edge. This is analogous to the failure mode of a sheet of paper compressed in an in-plane form from its edges. It is known from a coarse grain MC simulation that layered silicate sheets are flexible and intercalated sequentially, beginning at the outermost gallery of the layered nanostructure.[18]

Figure 5 shows the wide angle X-ray patterns of the fiber and the cast film. The X-ray patterns of the fiber [Fig. 5(a)] show several ordered reflections along the meridian. Strong equatorial reflections and several off-meridional reflections are also observed in Figure 5(a). The *d*-spacings of the meridional reflections are in the order of 12.9 Å (12.9/1, 12.9/2, 12.9/3, etc). The fiber repeat is the same as the reported value, indicating that the repeat unit is one monomer and that the CN-group is randomly substituted on the benzene ring.[19] Only even reflections such as 002, 004, 006 were observed in the well-ordered crystal because of the *n* glide plane and the 2_1 screw axis symmetry of the two chains in the unit cell.[19] An observation of the whole reflections, including odd reflections, indicated that the packing of the crystal was not perfect, although the presence of off-meridional reflections indicates that the chains are registered between the adjacent chains. The first strong reflection at $d = 21.4$ Å along the equator (the *d*-spacing will be discussed later) is due to the layered silicate. The equatorial position indicates that the normal of the surface of the layered silicate is oriented perpendicular to the chain axis. The narrow width of the azimuthal scan of this reflection means that the degree of orientation of the surface of layered silicates is quite good. Figure 5(b) shows the X-ray pattern of the film when the X-ray beam is parallel (TD pattern) to the film surface. The 00*l* reflections are parallel to the film surface, indicating that the chain axis is parallel to the film surface. A parallel orientation of the polymer chain in the film is usually observed for films made from the lyotropic liquid crystalline polymers. The scattering from the layered silicate is located perpendicular to the film surface. This is due to the parallel orientation of the layered silicate in the composite film, which coincides with the TEM result. The scattering extends to the origin of the X-ray pattern (the direct beam), perpendicular to the film surface. This streak may be due to the distribution of the larger gallery gap in the layered silicate, as shown in Figure 4. Figure 5(c) shows the X-ray pattern of the film when the X-ray beam is perpendicular (ND pattern) to the film surface. The 00*l* reflections are isotropic because the chains are randomly oriented along the film surface. The combined information of Figures 5(b) and 5(c) suggests that the polymer chains have a planar orientation. The scattering from the layered silicate is barely visible in Figure 5(c) because the scattering vector of the layered silicate is normal to the film surface and cannot be touched with the Ewald reflection sphere. The parallel orientation of the layered silicate in the film may influence the anisotropic film properties.

Figure 6 presents the one-dimensional X-ray data of the nanocompsite film. The scattering of the cloisite 30B occurs at $2\theta = 4.7°$ ($d = 18.7$ Å). The *d*-spacing represents the gap of the gallery in the layered silicate.

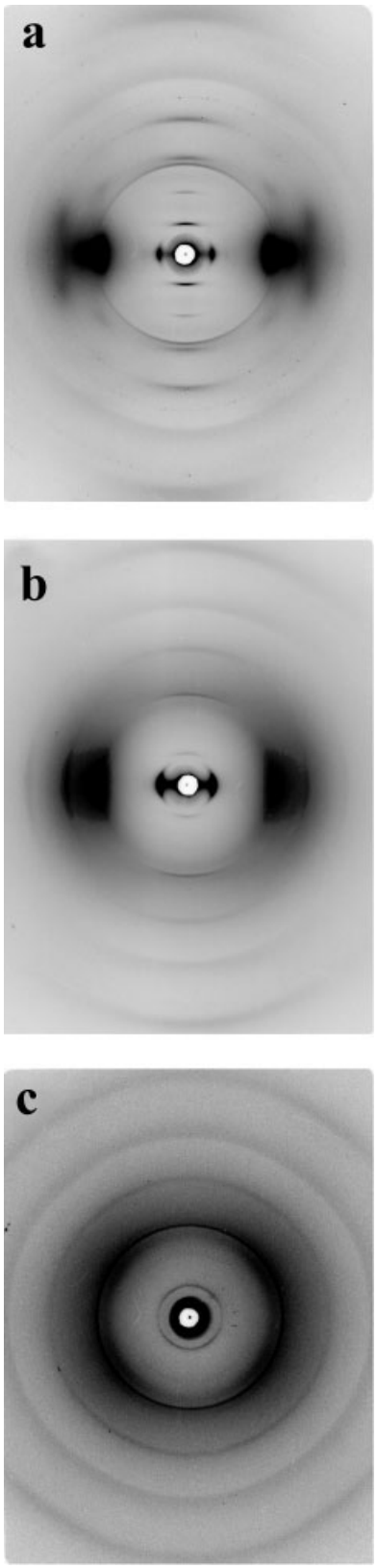

Figure 5 Wide angle X-ray patterns of (a) the fiber and the cast film with an X-ray beam of (b) ND and (c) TD directions; the vertical direction is parallel to the fiber axis in (a) and the film surface in (b).

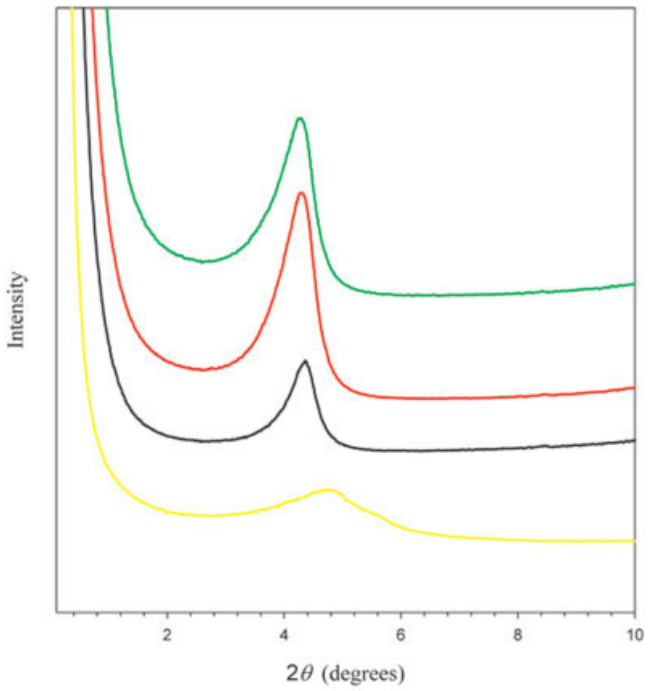

Figure 6 X-ray diffractograms of cloisite 30B and nanocomposites containing various amounts of layered silicate with a X-ray beam parallel to the film surface. Yellow, Cliosite 30B; black, CN-PPTA/5 wt % layered silicate; red, CN-PPTA/7.5 wt % layered silicate; green, CN-PPTA/10 wt % layered silicate. [Color figure can be viewed in the online issue, which is available at www.interscience.wiley.com.]

The peak of the layered silicate changes toward a lower angle at $2\theta = 4.1°$ ($d = 21.1$ Å) for the nanocomposite, indicating that the gallery opens up during an *in situ* synthesis of the nanocomposite. The increase in the *d*-spacing of the layered silicate means that the layered silicate is intercalated in the CN-PPTA/layered silicate nanocomposite and that it is not completely exfoliated during the *in situ* polymerization. It is difficult and theoretically impossible for the rigid polymers to penetrate the gallery of the layered silicate because of the large radius gyrations of the rigid polymers. The *in situ* polymerization method may be the only way to get the monomers into the gallery of the layered silicate and to polymerize them in the gallery, although the gap of the gallery did not increased much for the nanocomposite.

CONCLUSIONS

We successfully prepared a PLSN system using the soluble CN-PPTA. To prepare the PLSN system, the *in situ* polymerization method was used with organically modified clay (cloisite 30B, southern clay). The nanocomposite dope in the lyotropic state was spun into well-oriented fibers and could be cast easily into the film. The molecular weight of the CN-PPTA in the

PLSN seemed to be low compared with that of the conventional CN-PPTA, as inferred from the interpolation of the mechanical properties, although it is able to be improved by the process optimization. Thermal properties, such as degradation temperature and stability of the viscoelastic properties (storage and loss moduli) were comparable to the pure CN-PPTA, while the strength (and modulus) of the nanocomposite linearly increased with the amount of layered silicate. The intercalated structure was observed by transmission electron microscopy and X-ray diffraction with an increase in the *d*-spacing from 18.7 Å (the organically modified layered silicate; cloisite 30B) to 21.1 Å (nanocomposite). The layered silicate covered a large surface area and was well oriented in the fiber and film with the normal of the surface of the layered silicate perpendicular to the fiber axis and the surface of the film.

References

1. Giannelis, E. P. J Miner Met Mater Soc 1992, March, 28.
2. Okada, A.; Kawasumi, M.; Usuki, A.; Kojima, Y.; Kurauchi, T.; Kamigaito, O. Mater Res Soc Symp Proc 1990, 171, 45.
3. Usuki, A.; Kojima, Y.; Kawasumi, M.; Okada, A.; Kurauchi, T.; Kamigaito, O.; Deguchi, R. Polym Prepr Jpn 1990, 39, 2427.
4. Kojima, Y.; Okada, A.; Usuki, A.; Kawasumi, M.; Kurauchi, T.; Kamigaito, O.; Deguchi, R. Polym Prepr Jpn 1990, 39, 2430.
5. Kojima, Y.; Okada, A.; Kawasumi, M.; Okada, A.; Fukushima, Y.; Kurauchi, T.; Kamigaito, O. J Mater Res 1993, 8, 1185.
6. Usuki, A.; Koiwai, A.; Kojima, Y.; Kawasumi, M.; Okada, A.; Kurauchi, T.; Kamigaito, O. J Appl Polym Sci 1995, 55, 119.
7. Kojima, Y.; Usuki, A.; Kawasumi, M.; Odaka, A.; Kurauchi, T.; Kamigaito, O.; Kaji, K. J Polym Sci Part B: Polym Phys 1994, 32, 625.
8. Kojima, Y.; Usuki, A.; Kawasumi, M.; Okada, A.; Kurauchi, T.; Kamigaito, O.; Kaji, K. J Polym Sci Part B: Polym Phys 1995, 33, 1039.
9. Rebouillat, S.; Peng, J. C. M.; Donnet, J. B. Polymer 1999, 40, 7341.
10. Rebouillat, S.; Donnet, J. B.; Wang, T. K. Polymer 1997, 38, 2245.
11. Socci, E. P.; Thomas, D. A.; Eby, R. K.; Grubb, D. T.; Adams, W. W. Polymer 1996, 37, 5005.
12. Park, S. J.; Seo, M. K.; Ma, T. J.; Lee, D. R. J Colloid Interface Sci 2002, 252, 249.
13. Bair, T. I.; Morgan, P. W.; Killian, F. L. Macromolecules 1977, 10, 1396.
14. Oh, T. J.; Han, S. J.; Kim, S. G. J Korean Fiber Soc 1996, 33, 814.
15. Oh, T. J.; Jang, Y. S. J Korean Fiber Soc 1998, 35, 182.
16. Oh, T. J. U.S. Pat. (to Kolon) 5,728,799 (1995).
17. Hsu, S. L. C.; Chang, K. C. Polymer 2002, 43, 4097.
18. Sinsawat, A.; Anderson, K. L.; Vaia, R. A.; Farmer, B. L. J Polym Sci Part B: Polym Phys 2003, 41, 3272.
19. Park, S. Y.; Lee, S. W.; Oh, T. J.; Blackwell, J. Macromolecules 2005, 38, 3713.